Supplementary Information for

Three-dimensional Coherent X-ray Diffraction Imaging via Deep Convolutional Neural Networks

Longlong Wu[1,2]*, Shinjae Yoo[1], Ana F. Suzana[2], Tadesse A. Assefa[2,3], Jiecheng Diao[4], Ross J. Harder[5], Wonsuk Cha[5] and Ian K. Robinson[2, 4†]

[1]*Computational Science Initiative, Brookhaven National Laboratory, Upton, NY 11973, USA*

[2]*Condensed Matter Physics and Materials Science Department, Brookhaven National Laboratory, Upton, NY 11973, USA*

[3]*Stanford Institute for Materials and Energy Sciences, SLAC National Accelerator Laboratory, Menlo Park, California 94025, USA*

[4]*London Centre for Nanotechnology, University College London, London, WC1E 6BT, United Kingdom.*

[5]*Advanced Photon Source, Argonne, Illinois 60439, USA*

[*] lwu@bnl.gov, [†] irobinson@bnl.gov

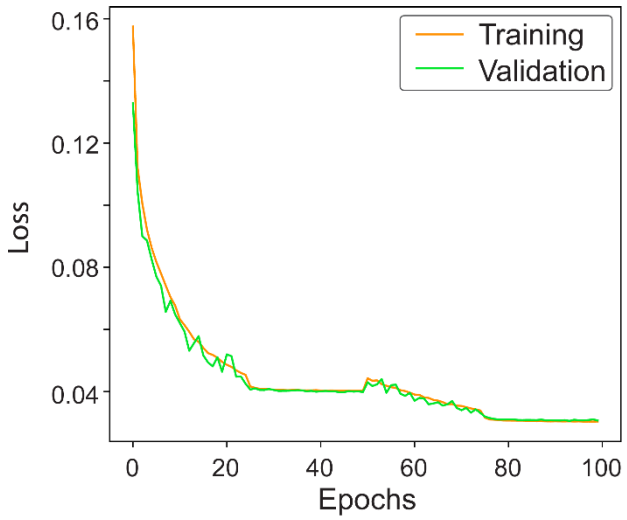

Supplementary Figure 1. Training and validation loss as a function of training epochs. The training and validation losses are almost the same because the training was stopped early to avoid overfitting.

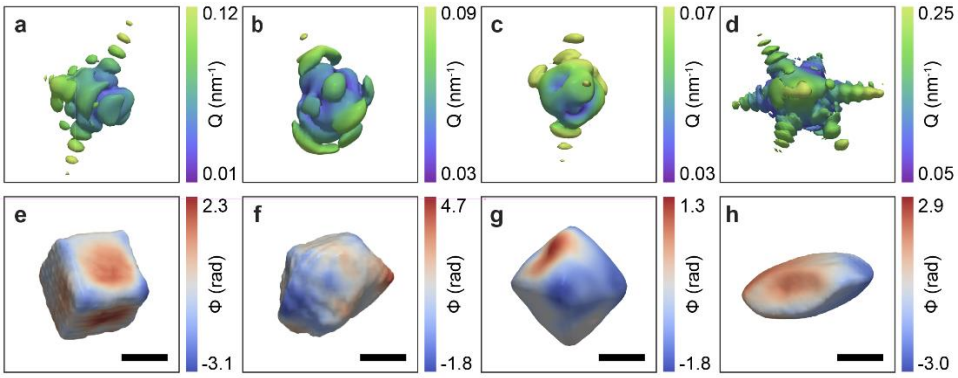

Supplementary Figure 2. Reconstructed results by applying the untrained 3D CNN model in unsupervised learning approach with randomly initialized bias and weight parameters to experimental data**.** (**a**)-(**d**) Isointensity plots of the 3D diffraction patterns of the predicted particles from the CNN model in reciprocal space, for $SrTiO_3$, $BaTiO_3$, Pd, and Au, respectively. The corresponding experimental 3D diffraction patterns are shown in Fig. 3(**a**)-(**d**). The colors correspond to the radial distance from the origin of reciprocal space. (**e**)-(**h**) The corresponding reconstructed real space particle structures from the model. In (**e**)-(**h**), the surface color encodes the complex phase values on the surfaces of these particle. All the scale bars are 150 nm.

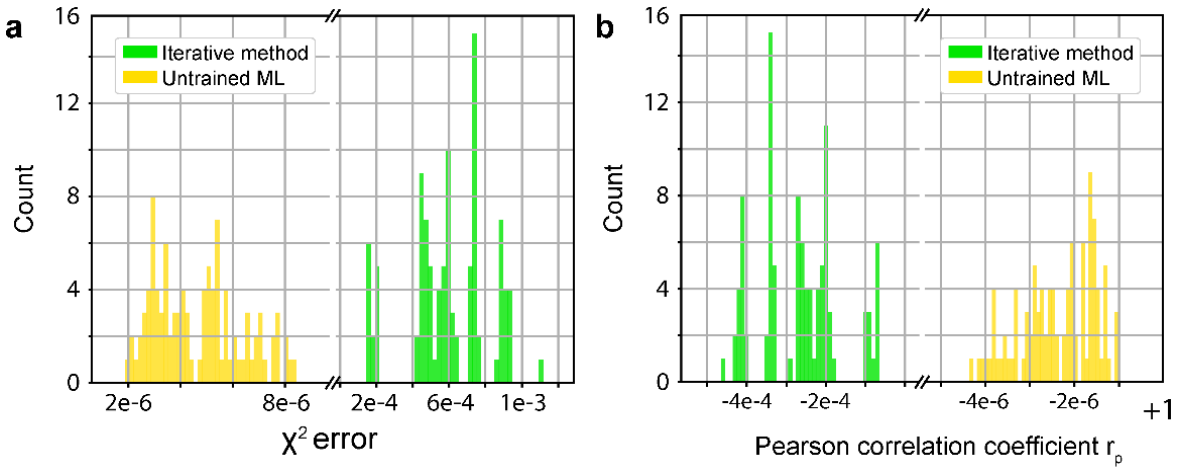

Supplementary Figure 3. Comparison of error metrics for two different methods with the simulated data in Fig 3. **a** Histogram of the observed χ^2 for the reconstructions from the conventional iterative method and the CNN model starting from randomly initialized weight and bias parameters. **b** The corresponding histogram of the Pearson correlation coefficient for both methods. The grouping of χ^2 values for the iterative algorithm is a well-known property of the HIO method jumping from one local minimum to the next. However, this trend is not obvious for the ML approach. Significantly, the obtained χ^2 error from the ML method is much smaller than that from the iterative method. The obtained r_p is also much closer to 1 than that from the iterative method.

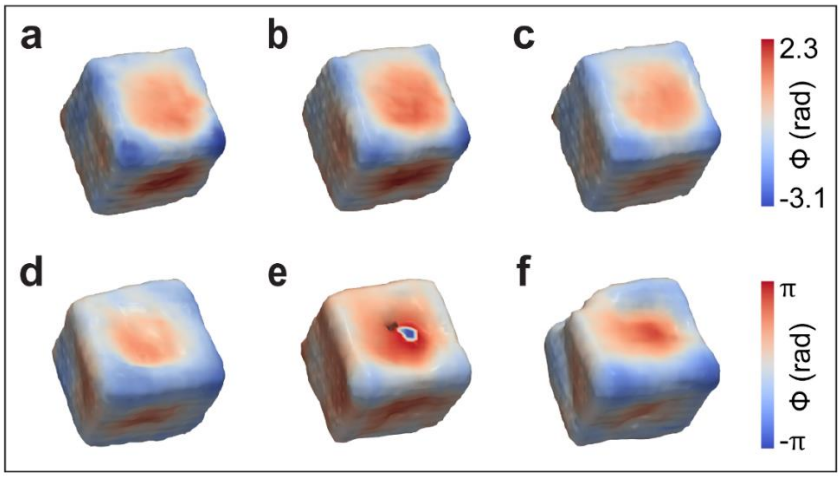

Supplementary Figure 4. Isosurface (15% contour level) comparison of the results from the untrained CNN model and the conventional iterative method. (**a**)-(**c**) Isosurface of the reconstructed $SrTiO_3$ particles with CNN model-based methods, colored according to the surface phase. For (**a**), the result was obtained by using the CNN model in unsupervised learning mode with the initial parameters from the trained CNN model. For (**b**)-(**c**), the results were obtained by using the CNN model in unsupervised learning mode with different random starting model parameters. (d)-(e) Reconstructions of the same data using the iterative method with alternations of ER and HIO algorithms starting from random distributions. A "shrinkwrap" support was applied using a 15% amplitude threshold. By comparing the reconstructed results from (**a**)-(**c**) with (**d**)-(**f**), it can be seen that the ML based methods give a better reproducibility of the shape and better fidelity to the presumed facetted cube shape. Furthermore, due to the phase of the reconstructed particles being restricted to the range $[-\pi, \pi]$ in the iterative method, sudden wraps of phase sometimes occur, as seen in (**e**). However, for the ML-based approach, there is no such limitation of the phase range.

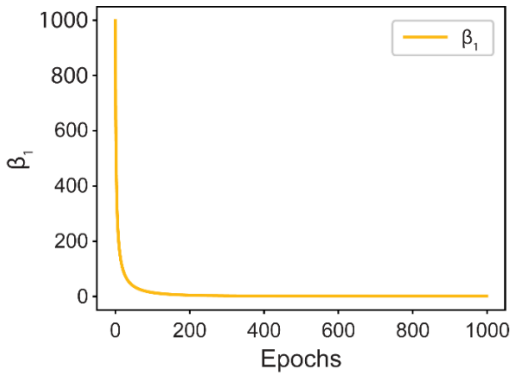

Supplementary Figure 5. Prescription for setting the weight parameter β_1 using the Weibull distribution in Eq. (7) as a function of training epochs during unsupervised ML approach.